

DTIC FILE COPY

Best Available Copy ②

REPORT DOCUMENTATION PAGE

REPORT DOCUMENTATION PAGE		Form Approved OMB No. 0704-0188	
1. REPORT NUMBER AD-A225 608		2. RESTRICTIVE MARKINGS	
3. DISTRIBUTION/AVAILABILITY OF REPORT Distribution unlimited		4. MONITORING ORGANIZATION REPORT NUMBER NA	
5. NAME OF PERFORMING ORGANIZATION Weizmann Institute of Science		6. NAME OF MONITORING ORGANIZATION Office of Naval Research	
7. ADDRESS (City, State, and ZIP Code) Dept. of Membrane Research The Weizmann Institute of Science Rehovot 76100, ISRAEL		8. ADDRESS (City, State, and ZIP Code) 800 N. Quincy St. Arlington, VA 22217-5000	
9. NAME OF PERFORMING ORGANIZATION Office of Naval Research		10. OFFICE SYMBOL (if applicable) ONR	
11. PROGRAM ELEMENT NUMBER N00014-37-G 0203		12. PROGRAM ELEMENT NUMBER 61153N	
13. PROJECT NUMBER BR04108		14. TASK NUMBER 441K713	
15. REPORT NUMBER 61153N		16. REPORT NUMBER BR04108	
17. REPORT NUMBER 441K713		18. REPORT NUMBER 61153N	
19. TITLE (Include Security Classification) Electric field dependence of protein conformation and channel function in lipid membrane of different compositions.			
20. AUTHOR (Last Name, First Name) Israel R. Miller			
21. DATE OF REPORT (Year, Month, Day) 1990			
22. DATE OF REPORT (Year, Month, Day) 1990			
23. DATE OF REPORT (Year, Month, Day) 1990			
24. DATE OF REPORT (Year, Month, Day) 1990			
25. DATE OF REPORT (Year, Month, Day) 1990			
26. DATE OF REPORT (Year, Month, Day) 1990			
27. DATE OF REPORT (Year, Month, Day) 1990			
28. DATE OF REPORT (Year, Month, Day) 1990			
29. DATE OF REPORT (Year, Month, Day) 1990			
30. DATE OF REPORT (Year, Month, Day) 1990			
31. DATE OF REPORT (Year, Month, Day) 1990			
32. DATE OF REPORT (Year, Month, Day) 1990			
33. DATE OF REPORT (Year, Month, Day) 1990			
34. DATE OF REPORT (Year, Month, Day) 1990			
35. DATE OF REPORT (Year, Month, Day) 1990			
36. DATE OF REPORT (Year, Month, Day) 1990			
37. DATE OF REPORT (Year, Month, Day) 1990			
38. DATE OF REPORT (Year, Month, Day) 1990			
39. DATE OF REPORT (Year, Month, Day) 1990			
40. DATE OF REPORT (Year, Month, Day) 1990			
41. DATE OF REPORT (Year, Month, Day) 1990			
42. DATE OF REPORT (Year, Month, Day) 1990			
43. DATE OF REPORT (Year, Month, Day) 1990			
44. DATE OF REPORT (Year, Month, Day) 1990			
45. DATE OF REPORT (Year, Month, Day) 1990			
46. DATE OF REPORT (Year, Month, Day) 1990			
47. DATE OF REPORT (Year, Month, Day) 1990			
48. DATE OF REPORT (Year, Month, Day) 1990			
49. DATE OF REPORT (Year, Month, Day) 1990			
50. DATE OF REPORT (Year, Month, Day) 1990			
51. DATE OF REPORT (Year, Month, Day) 1990			
52. DATE OF REPORT (Year, Month, Day) 1990			
53. DATE OF REPORT (Year, Month, Day) 1990			
54. DATE OF REPORT (Year, Month, Day) 1990			
55. DATE OF REPORT (Year, Month, Day) 1990			
56. DATE OF REPORT (Year, Month, Day) 1990			
57. DATE OF REPORT (Year, Month, Day) 1990			
58. DATE OF REPORT (Year, Month, Day) 1990			
59. DATE OF REPORT (Year, Month, Day) 1990			
60. DATE OF REPORT (Year, Month, Day) 1990			
61. DATE OF REPORT (Year, Month, Day) 1990			
62. DATE OF REPORT (Year, Month, Day) 1990			
63. DATE OF REPORT (Year, Month, Day) 1990			
64. DATE OF REPORT (Year, Month, Day) 1990			
65. DATE OF REPORT (Year, Month, Day) 1990			
66. DATE OF REPORT (Year, Month, Day) 1990			
67. DATE OF REPORT (Year, Month, Day) 1990			
68. DATE OF REPORT (Year, Month, Day) 1990			
69. DATE OF REPORT (Year, Month, Day) 1990			
70. DATE OF REPORT (Year, Month, Day) 1990			
71. DATE OF REPORT (Year, Month, Day) 1990			
72. DATE OF REPORT (Year, Month, Day) 1990			
73. DATE OF REPORT (Year, Month, Day) 1990			
74. DATE OF REPORT (Year, Month, Day) 1990			
75. DATE OF REPORT (Year, Month, Day) 1990			
76. DATE OF REPORT (Year, Month, Day) 1990			
77. DATE OF REPORT (Year, Month, Day) 1990			
78. DATE OF REPORT (Year, Month, Day) 1990			
79. DATE OF REPORT (Year, Month, Day) 1990			
80. DATE OF REPORT (Year, Month, Day) 1990			
81. DATE OF REPORT (Year, Month, Day) 1990			
82. DATE OF REPORT (Year, Month, Day) 1990			
83. DATE OF REPORT (Year, Month, Day) 1990			
84. DATE OF REPORT (Year, Month, Day) 1990			
85. DATE OF REPORT (Year, Month, Day) 1990			
86. DATE OF REPORT (Year, Month, Day) 1990			
87. DATE OF REPORT (Year, Month, Day) 1990			
88. DATE OF REPORT (Year, Month, Day) 1990			
89. DATE OF REPORT (Year, Month, Day) 1990			
90. DATE OF REPORT (Year, Month, Day) 1990			
91. DATE OF REPORT (Year, Month, Day) 1990			
92. DATE OF REPORT (Year, Month, Day) 1990			
93. DATE OF REPORT (Year, Month, Day) 1990			
94. DATE OF REPORT (Year, Month, Day) 1990			
95. DATE OF REPORT (Year, Month, Day) 1990			
96. DATE OF REPORT (Year, Month, Day) 1990			
97. DATE OF REPORT (Year, Month, Day) 1990			
98. DATE OF REPORT (Year, Month, Day) 1990			
99. DATE OF REPORT (Year, Month, Day) 1990			
100. DATE OF REPORT (Year, Month, Day) 1990			

Best Available Copy

Final Report on Contract N00014-87-G-0203**Principal Investigator : Israel R. Miller****Title: Electrical field dependence of protein conformation mobility and channel function in lipid membranes of different compositions.****Research Objectives:**

The objective is to study the effect of cross membrane electric fields on membrane permeability and on the conformation of membrane lipids, proteins and channel forming polypeptides. Another objective is to study the tangential field dependence of the lateral mobility of membrane components. The combined effort was aimed to gain insight and the mechanism of functioning of channels and of signal transducing receptors.

The research has been conducted on model system, namely lipid monolayers and lipid bilayer membranes.

Accomplishments during the three years of research**1. Interactions with lipid monolayers on the polarized mercury electrode surface.****a. Interactions in the lipid head group region and their effect on the monolayer structure and permeability.**

We demonstrated that interactions in the headgroup region without any appreciable hydrophobic contribution may change the lipid layer structure rendering it permeable to ions. This is brought about by expanding the area of the head group region which is then bound to invaginate into the hydrocarbon layer. The phenomenon was illustrated by following examples:

1. Furosemide which is quite a polar diuretic anion (acting on the ascending segment of the loop of Henle) [1] was shown to penetrate the head group region of monolayers of phosphatidylcholine (PC), phosphatidylethanolamine (PE) and mixtures of PC with bovine brain sphingomyelin (SM). Furosemide, when intercalated between the headgroups, expands the area of the polar layer with concomitant decrease in the thickness of the hydrocarbon layer. This decrease in dielectric thickness results in increased differential capacitance [2]. At higher concentrations and at positive polarization of the mercury surface the furosemide anion tends to penetrate the lipid monolayer and adhere to the positively charged surface with a concomitant abrupt increase in capacitance. The increase in capacitance and the monolayer penetration is considerably larger in the Zwitterionic non hydrogen bonded monolayers of PC and of SM than in monolayers of PE which contains strong intermolecular hydrogen bonds (see Fig. 1). The penetration of the monolayer by furosemide facilitates the electrode reactions which are inhibited by the monolayer. The reduction currents of oxygen across the monolayer is enhanced by furosemide. The current increases abruptly at the potential at abrupt increase in capacitance. However, at still more positive potentials where the negatively charged furosemide is strongly adsorbed after displacing the lipid it inhibits the electron transfer and thus the reduction of oxygen.

2. The ganglioside GM₁ is a specific receptor for cholera toxin (CT) and GT₁ is a specific receptor for tetanotoxin (TeT) [3]. Phospholipid monolayers containing as little as 1% GM₁ show upon interaction with CT at concentrations below 0.6 µg/ml a nearly three fold increase in capacitance and a five fold increase in reduction current of Cu²⁺. If instead of GM₁ another ganglioside e.g. GT₁ is added to the monolayer, the monolayer does not interact with CT and its capacitance or permeability is not affected. The effect of TeT on the capacitance and permeability of the monolayers containing GT₁ is smaller than that of CT on GM₁ containing monolayers but still the effect very specific. TeT does not affect lipid monolayers containing other gangliosides. All this is

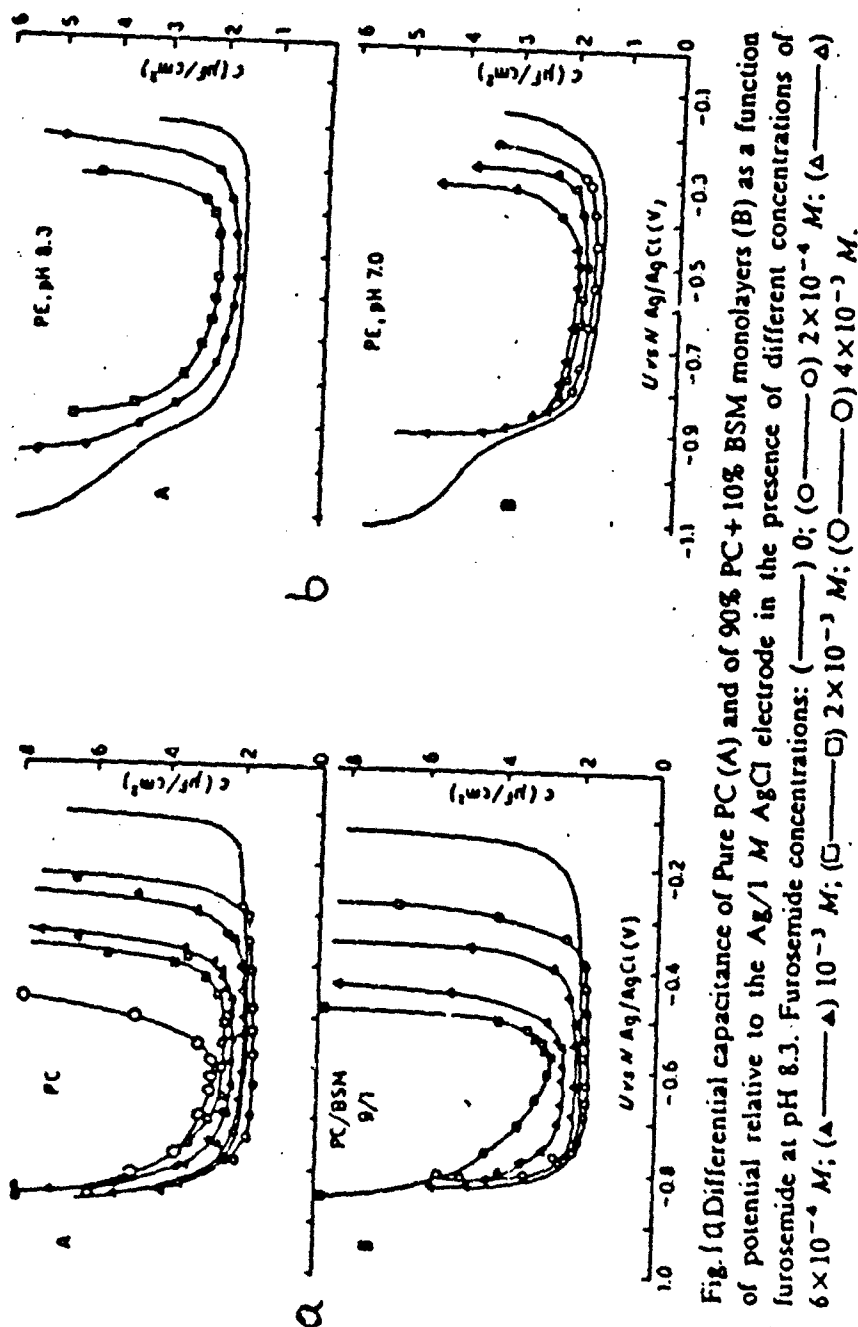


Fig. 1a Differential capacitance of Pure PC (A) and of 90% PC + 10% BSM monolayers (B) as a function of potential relative to the Ag/1 M AgCl electrode in the presence of different concentrations of furosemide at pH 8.3. Furosemide concentrations: (—) 0; (O) 2×10^{-4} M; (\square) 2×10^{-3} M; (Δ) 4×10^{-3} M; (\bullet) 6×10^{-3} M.

Fig. 1b Differential capacitance of PE monolayers at pH 8.3 (A) and at pH 7 (B) as function of potential relative to the Ag/1 M AgCl electrode. Furosemide concentrations: (—) 0; (u) 2.15×10^{-3} M; (Δ) 4.3×10^{-3} M; (\bullet) 8.6×10^{-3} M; (\bullet) 4×10^{-3} M; (\bullet) 1.2×10^{-2} M.

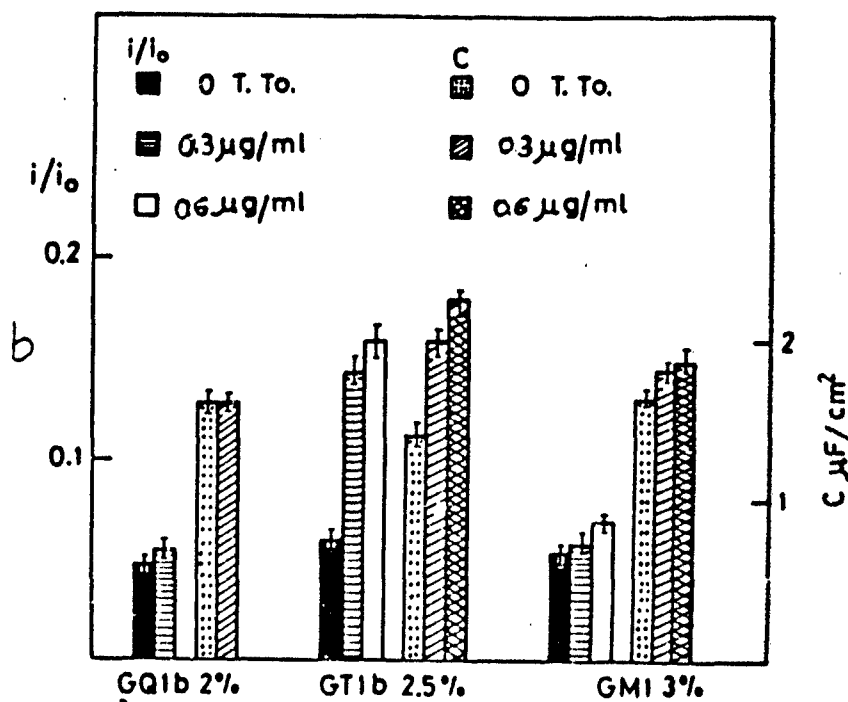
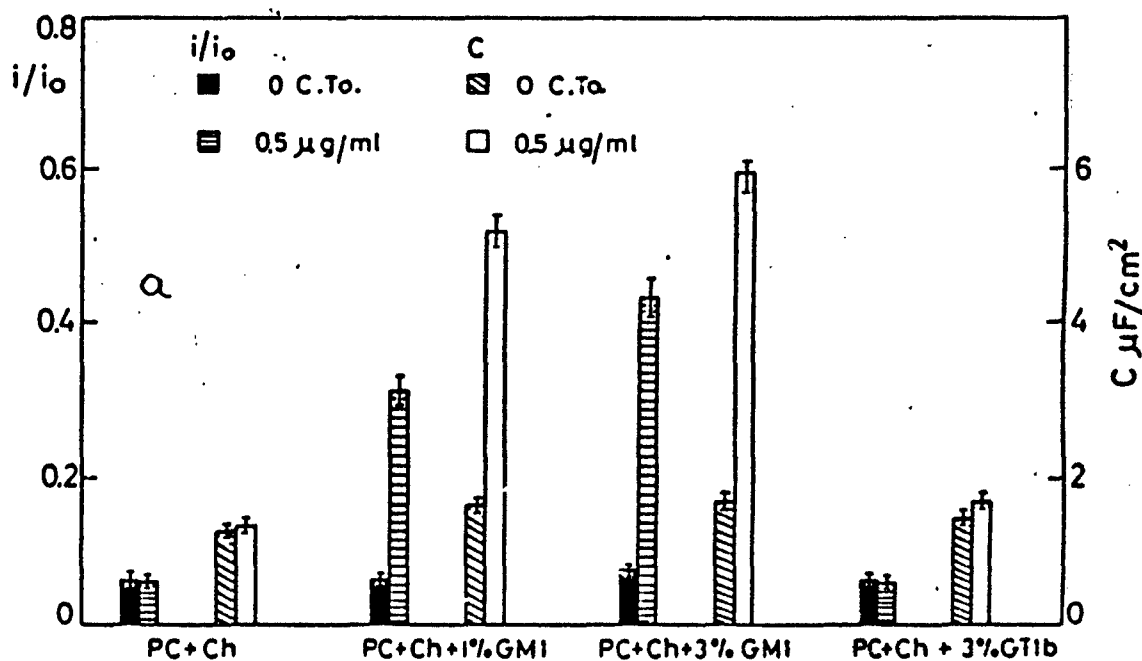


Fig. 2. a. Histogram illustrating the large effect of GM_1 on the capacitance and the ionic permeability of GM_1 containing monolayers in contrast to monolayers containing GT_1 or no gangliosides at all.
b. Effect of TeT on monolayers containing GT_1 .

Accession For	
NTIS GRA&I	<input checked="" type="checkbox"/>
DTIC TAB	<input type="checkbox"/>
Unannounced	<input type="checkbox"/>
Justification	
By _____	
Distribution/	
Availability Codes	
Dist	Avail and/or Special
A-1	

illustrated in Fig. 2a and b where the capacitances and the reduced currents (current divided by the maximal diffusion current) at the potential of the maximal stability of the monolayer are given. In parallel the negligible effects of the non specific gangliosides are shown.

The specific interaction of the toxins is with the head groups of the gangliosides. The toxins are composed of subunits and each of the binding subunits contains one binding site. Ultimately about five ganglioside molecules can bind to one toxin molecule. Such a complex, in order to be sterically feasible has to have the protein in the middle with the ganglioside molecules surrounding it. This conformation in the surface layer is bound to perturb the continuity of the hydrocarbon layer to induce high capacitance and high conductance parallel elements.

iii. Protein kinase C (PKC) is active on membrane surface and its activity is affected by the presence of phorbol ester which is a tumor promoting agent (TPA) and by diacylglycerol (DAG) [4]. We employed the electrodic response of its cysteine groups on a bare and at lipid monolayer covered mercury electrode to look for a clue whether conformational changes are related to its activation. The accessibility of the 5-6 cysteine disulfide bonds of PKC for reduction on the mercury electrode served as a criterion for conformational changes in its tertiary structure when interacting with the different interfaces [5]. Two major reduction peaks of cystine at different microenvironments within the protein adsorbed on a mercury surface were observed at two distinct potentials in the a.c. polarograms and in the cyclic voltamograms. As protons are required for the reduction of cystine to cysteine the reduction peaks shift to negative potentials as the pH of the solution is increased (Fig. 3a). The peak at the more positive potential (-0.46V at pH 7.4) evolves when the respective cystine residues are allowed sufficient to get adsorbed before getting reduced. After their reduction they tend to leave the surface as the affinity of their microenvironment to the mercury surface is low. The more negative peak at -0.62V is obtained after short exposure to the surface and its size is not diminished after reduction and reoxidation indicating that it is in a surface active environment. Ca^{2+} and Mg^{2+} have only negligible effects on the peaks. PKC penetrates phospholipid monolayers to some extent. Addition of DAG or TPA to these monolayers facilitates their penetration. These compounds stabilize the protein surface conformation which exposes to the electrode the cystine residues which are reduced at the more positive potentials (0.42 V) (Fig. 3b). This phenomenon is not significantly affected by Mg^{2+} or by Ca^{2+} .

b. Adsorption of hydrophobic channel forming polypeptides alamethicin and melittin at the mercury/water interface and their penetration of phospholipid monolayers at these interfaces.

The differential capacitance of condensed monolayers of phosphatidylcholine (PC) or of mixtures of PC with phosphatidylserine at the mercury/water interface was measured in the presence of different concentrations of the antibiotic alamethicin or of the bee venom component melittin [6,7]. The degree of perturbation of the structure of the phospholipid monolayers and their penetration by the oligopeptides was inferred from the increase in differential capacity and from their suppressed impedance to polarographic currents carried by ionic depolarizer. The augmentation of the capacitance and of the ionic permeability depends not only on the degree of penetration or of displacement of the lipid monolayer by the oligopeptides but also by the surface properties of the displaced domains. Alamethicin is much more hydrophobic than melittin. Alamethicin adsorbs on the mercury surface giving a condensed monolayer of a minimal specific capacitance $< 4 \mu\text{f}/\text{cm}^2$ from concentrations $< 1 \mu\text{g}/\text{ml}$. It hinders the access of ions to the electrode surface suppressing the pseudocapacitance peak of Tl^+ to less than half of its value without the monolayer and it practically eliminates the pseudocapacitance of Cd^{++} . Cyclic voltamograms show scan rate dependent shifts in peak potentials characteristic for ionic permeability of the surface layer. Thus, even high degrees of penetration or displacement of lipid monolayers by alamethicin has only a moderate effect on the monolayer capacitance and permeability.

In Fig. 4a the effect of alamethicin on the capacitance and on the permeability to Tl^+ of a phosphatidylcholine monolayer is shown. The effect increases at relatively short times of exposure of the monolayer covered electrode to the alamethicin containing solution. It decreases at longer times until the monolayer capacitance and the Tl^+ pseudocapacitance peak (indicative of monolayer permeability to Tl^+) reach to

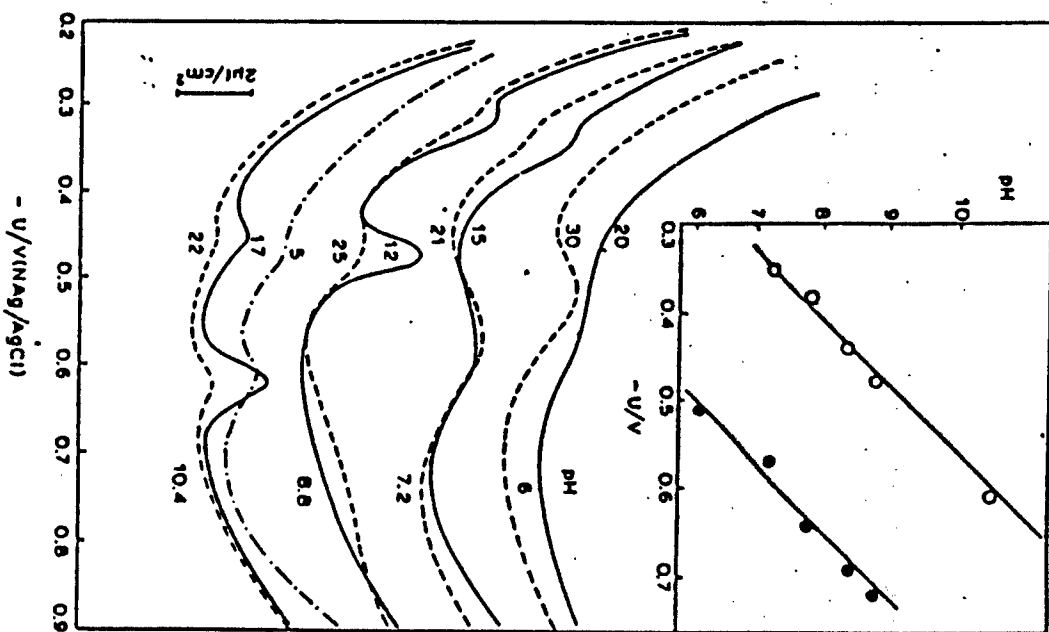


Fig. 3a Differential capacitance curves in the presence of adsorbed PKC at different pH values. Adsorption from a solution of 1 μg per ml PKC in 0.1 M KCl, 0.5 mM EGTA. Two to three curves at the indicated adsorption times were recorded at each of the four pH values. The inset represents the potentials of the two main peaks as a function of pH. O, represents the peak at -0.4 V and the ●, represents the peak at $+0.6$ V, measured at pH 7.4; $-U/V$ is as defined in Fig. 2.

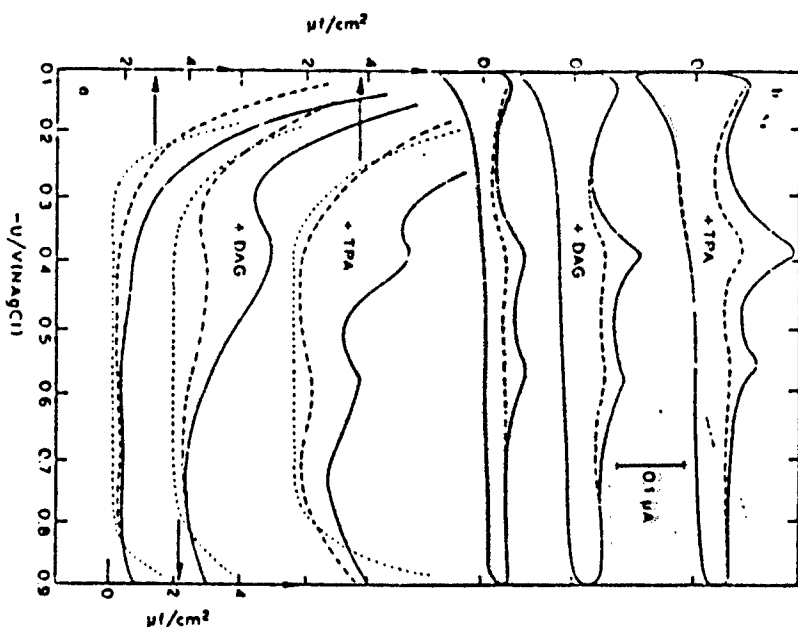


Fig. 3b Dielectric reaction of PKC across a pure phosphatidylserine (PS) monolayer and a PS monolayer containing 10% DAG or 0.5% TPA. The monolayers were spread on a 1 $\mu\text{g}/\text{ml}$ PKC solution. 30 min after spreading, the monolayer with the interacting PKC was transferred to the surface of a newly formed hanging mercury drop. 10 min after deposition of the monolayer complex on the electrode consecutive a.c. polarograms or cyclic voltammograms were recorded. (a) Differential capacitance curves: —, monolayers in the absence of PKC; —, first scan in the presence of PKC; and —, — third of fourth scan when the polarograms reached a final shape. (b) Cyclic voltammograms: —, first scan; and —, a subsequent scan when the voltammograms did not undergo additional change. Similar a.c. polarograms and cyclic voltammograms (S.E. 55%) were obtained for samples in the presence of Ca^{2+} (100 μM) and Mg^{2+} (1 mM). $-U/V$ is defined as in Fig. 2.

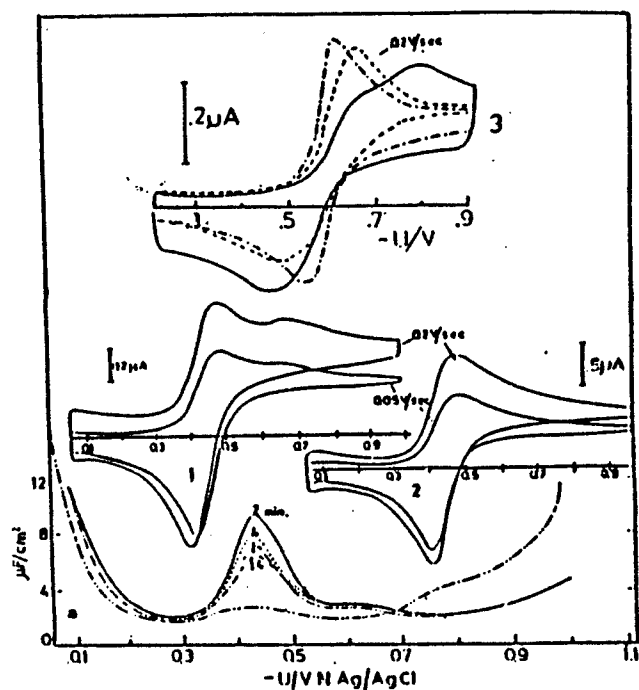


FIGURE 4. Differential capacitance curves of PC monolayer in the presence of alamethicin ($0.4 \mu\text{g}/\text{cm}^2$)

PC spread over a solution containing $1 \mu\text{g}/\text{ml}$ alamethicin.

The hanging drop was formed across the monolayer and immersed into the solution 20 minutes after spreading the monolayer ($0.4 \mu\text{g}/\text{cm}^2$). The first polarogram was started immediately and completed within 12 seconds. Every consecutive minute a new ac polarogram was recorded, some of them are presented. The polarogram obtained at the 14th scan did not change any more.

- - - polarogram without alamethicin in the solution.

Inserts: Cyclic voltammograms (CV) after transfer of the PC monolayer ($0.4 \mu\text{g}/\text{cm}^2$) onto the electrode surface.

Insert 1: CV without alamethicin in solution with $4 \cdot 10^{-5} \text{M}$ Ti^{4+} .

Insert 2: CV with $1 \mu\text{g}/\text{ml}$ alamethicin in the solution, 13 minutes after the transfer of the PC monolayer onto the electrode.

Insert 3: CV of PC monolayers in the presence of $4 \cdot 10^{-5} \text{M}$ Cd^{2+} .

— without alamethicin.

— $1 \mu\text{g}/\text{ml}$ alamethicin 1 min after transfer of the monolayer onto the electrode surface.

- - - 10 min after the transfer of the monolayer.

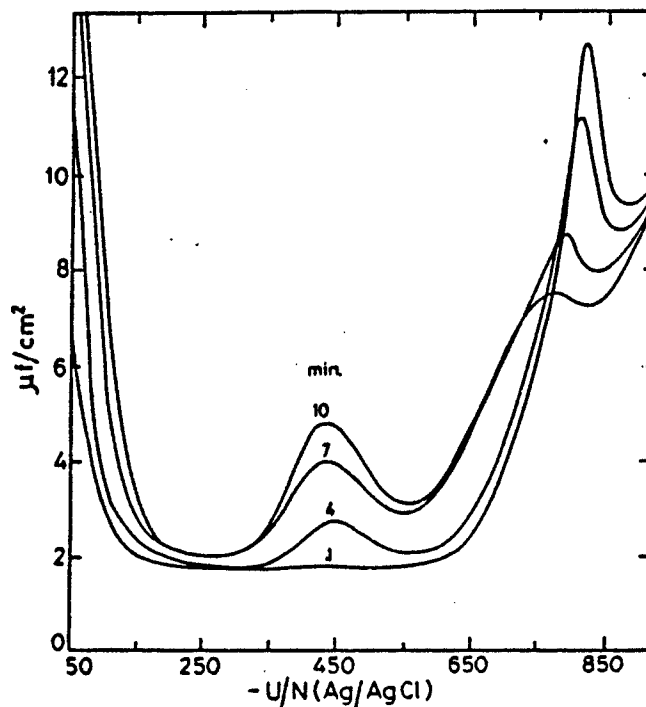


FIGURE 5. Differential capacitance curves of a PC monolayer in the presence of melittin ($0.4 \mu\text{g}/\text{cm}^2$)

PC spread over a solution containing $2 \mu\text{g}/\text{ml}$ melittin and $4 \cdot 10^{-5} \text{M}$ Ti^{4+} .

The polarograms recorded at different times after transfer of the monolayer onto the electrode surface as indicated.

The monolayer was transferred 20 min after its spreading by formation of a hanging mercury drop across the monolayer.

Best Available Copy

values obtained in the absence of alamethicin. Cyclic voltametry shows (Fig. 4) that it is the reduction current depending on the transport of Tl^+ ions across the monolayer to the electrode, which is predominantly impeded. Another reduction peak around 0.1V appears besides the one around -0.45V. The function reduced at -0.1V increases with the monolayer impedance on top of the slight negative shift of the -0.45V peak. The reoxidation rate of metallic Tl to Tl^+ (anodic peak) is only slightly affected by the monolayer and by the change of its impedance.

Melittin on the other hand is a relatively hydrophilic molecule with a substantial positive net charge. The minimal capacitance of its condensed adsorbed monolayer is around 9 to 10 $\mu f/cm^2$ and in spite of its positive net charge it is almost freely permeable to Tl^+ without lowering its diffusion current or its pseudocapacitance peak when reduced on the electrode surface. It perturbs only little the structure of lipid monolayers at positive polarizations as it cannot properly penetrate the lipid monolayer without exposing polar groups to its hydrophobic domain. The penetration is more pronounced at negative polarization when the positive polarizations of melittin are attracted by the negative surface charges (Fig. 5).

2. Effect of the channel formers melittin and alamethacin and of CT-GM₁ complexes on the ionic permeability of vesicular lipid bilayer membranes.

In these experiments large vesicles of radii between 80 and 150 nm were used. These were obtained by injection of solution of the phospholipids in pentane [8] into the aqueous solution containing 0.1M salt of the electroactive ion, e.g. $CdSO_4$, $Tl_2^+SO_4$, KJO_3 at 60°C. The electroactive salt in the external solution was replaced with nonelectroactive one by exhaustive dialysis against the respective salt solution at the same concentration. The release of the electroactive ions from the vesicles was measured after further dilution by pulse polarography [9]. The procedure is exemplified in Fig. 6. The pulse polarograms of the pure buffered salt solution and after adding 0.1 ml of the vesicular suspension (~2 mg lipid/ml) to 10 ml of the solution, were recorded first. At the final negative potential the recorder was transferred to the time base. Different quantities of alamethicin or melittin or of cholera or tetanotoxin when the vesicles contained the respective gangliosides, were added at the time indicated. The increase of current with time was then recorded. In some experiments the polypeptides were diluted in the polarographic cells before adding the vesicles, in order to avoid any contact of the vesicles with concentrated membrane perturbing peptides.

a. Release of ions by channel forming polypeptides.

In spite of the difference in hydrophobicity the effect of the two channel formers, alamethicin and melittin, is comparable even though alamethicin acts on release of the electroactive cations at lower concentrations. As evident from Figs. 7 and 8, the rate of release by the two polypeptide does not depend only on their final concentration in solution but also on the concentration of the solution added to the vesicle suspension. The higher is the concentration of the polypeptide added to the suspension the more effective the release even though the final concentration and the number of molecules acting on the vesicles is the same. This behavior was observed in all channel forming polypeptides which show lytic activity. Paradaxin, which is a short repellent and a channel former without any appreciable lytic activity, releases ions from vesicles at a given concentration at the same rate, no matter what was the concentration of the solution added to the suspension.

The permeability to the large anion IO^{-3} is generally smaller than to the smaller cations Tl^+ and Cd^{2+} . Even melittin which is positively charged and is supposed to be selective to anion is slightly more permeable to Tl^+ than to IO^{-3} . In the case of alamethicin the permeability to Cd^{2+} is nearly 10 fold larger than that to IO^{-3} (Fig. 8). In either case the permeability is smaller when SO_4^{-2} rather than Cl^- , Br^- or NO_3^- , are the other anions in the system. This stresses the importance the cotransport of the counter ion and counter transport of the cation in the measured permeability of the electroactive ion.

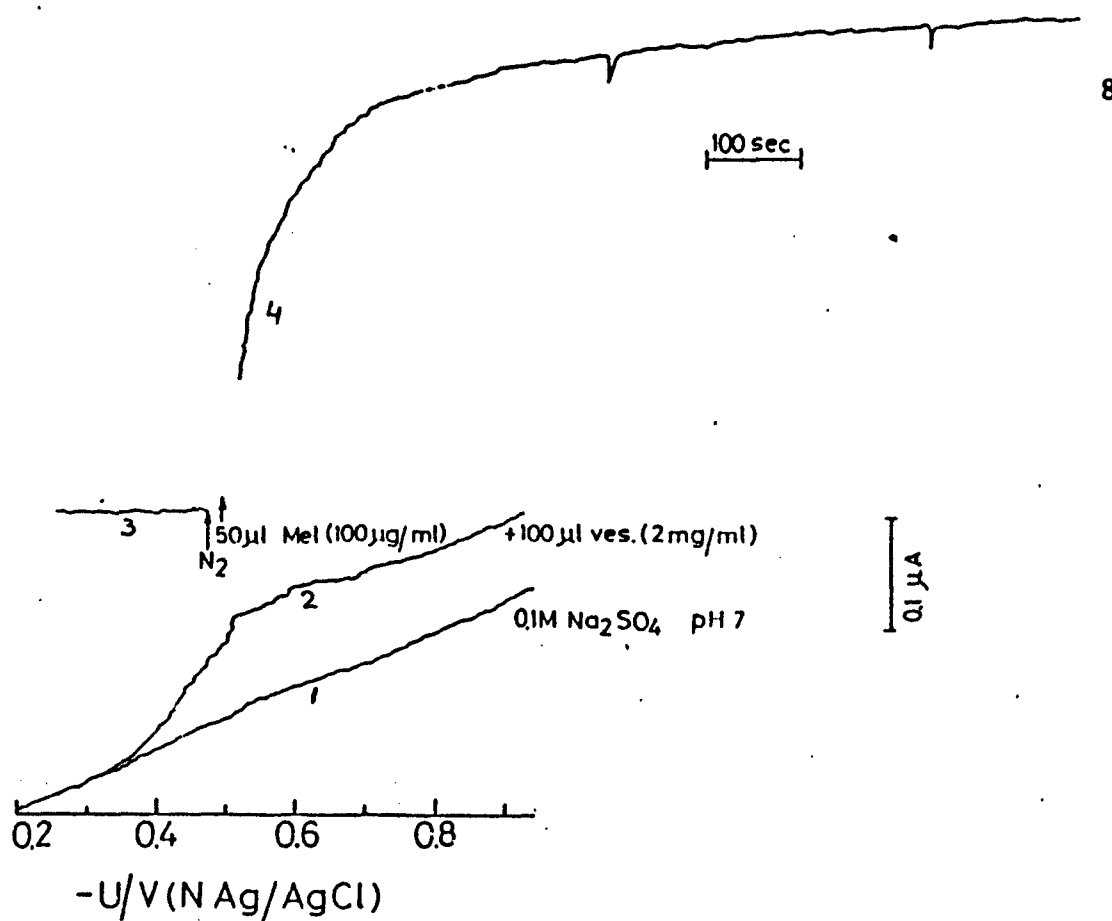


Figure 6 Experimental procedure for determination of the kinetics of release of electroactive ions (Tl^+ in the case demonstrated) from vesicles by pulse polarography:

Step 1: Pulse polarogram in the presence of buffered salt solution

Step 2: Pulse polarogram after addition of 100 μ l of concentrated vesicle suspensions. The half wave potential at -0.45V relative to Na-Ag/AgCl electrode and the diffusion current are due to the Tl^+ concentration not removed by dialysis and remaining in the extravascular phase.

Step 3: The recorder is set on the time base holding the final potential (-0.95V).

Step 4: To the solution, stirred by a stream of N_2 aliquots of concentrated solution of the polypeptide was added to reach the final desired concentration.

In some experiments the concentrated suspension of vesicles was added to the solution containing the polypeptide at its nearly final concentration.

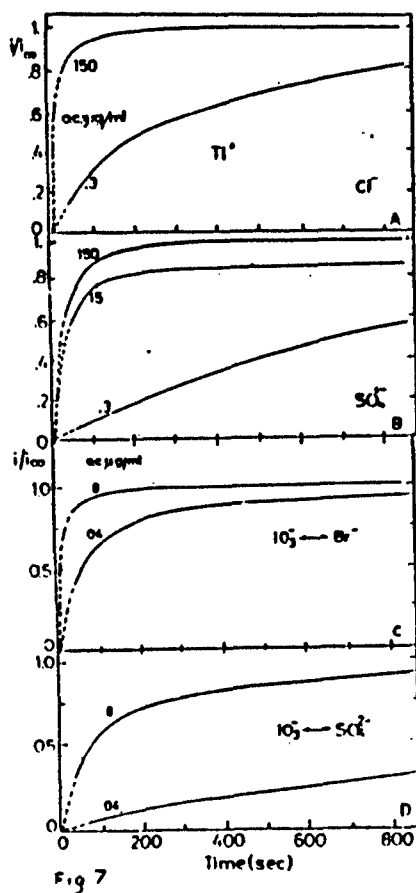


Fig 7

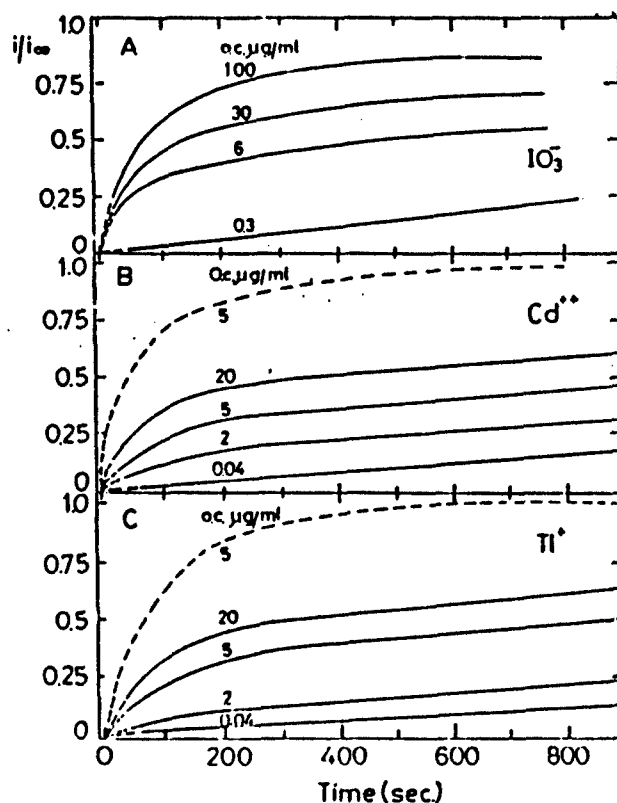


Fig 8

Figure 7. Dependence of the release kinetics through melittin channels on the salt composition in the extravesicular phase, at pH 7.

The original concentration (o.c.) of melittin in the added solution indicated.

Final concentrations A and B 0.3 µg/ml, C and D 0.4 µg/ml.

A: Tl^+ release measured, NaCl in outer phase, B: Tl^+ release measured, Na_2SO_4 in outer phase.

C: IO_3^- release measured, NaBr in outer phase.

D: IO_3^- release measured, Na_2SO_4 in outer phase.

Figure 8. Release kinetics of Tl^+ , Cd^{2+} and IO_3^- by alamethicin at pH 7.

The original concentrations (o.c.) of the added alamethicin solution indicated. The final concentrations:

for the release of Tl^+ and Cd^{2+} : full line 0.04 µg/ml, wide dashed lines 0.1 µg/ml; for the release of IO_3^- 0.3 µg/ml.

0.1M Na_2SO_4 in the extravesicular phase. (There is no appreciable change with pH between pH 5.5 and pH 8).

Best Available Copy

b. Inducement of leakage by GM_1 CT and GT_1 TeT complexes.

In spite of the pronounced perturbation of the continuity of lipid monolayers on the mercury surface, the CT- GM_1 or the TeT- GT_1 complexes do not induce any appreciable leakage of ion from vesicles. Outside positive membrane incorporate the complexes into the bilayer and facilitate the release of Tl^+ . The outside positive membrane potential is obtained by low concentrations ($2 \cdot 10^{-9}$ - $5 \cdot 10^{-8}M$) of valinomycin which binds and transports the Tl^+ from inside than the Na^+ from outside. The effect of the potential on the release is illustrated in Fig. 9. If K_2SO_4 instead of Na_2SO_4 is in the outer solution, added valinomycin induces leakage alone as it can transport Tl^+ out while transporting K in. The rate of transport is not increased by added CT. Complexes of TeT with GT_1 behave similarly.

3. Effect of membrane potentials or crossmembrane electric fields on the conformation of membrane proteins and polypeptides

The changes in conformation of bacteriorhodopsin and of alamethicin incorporated in lipid bilayers was obtained from the change in the measured circular dichroism (CD) in the peptide adsorption region between 190 and 250 nm. The membrane potential in the case of bacteriorhodopsin embedded in the bilayer membranes of lipid vesicles was monitored by potassium gradient across the membrane and valinomycin. This method was not applicable to alamethicin which introduces leakiness and shortcircuits the membrane. In this last case we created Douvian potential across the membrane, using Na-polyacrylate on one side of the membrane with different salt concentrations on the other side. The osmotic pressure was ballanced by glucose.

The CD spectra of both of bacteriorhodopsin and of alamethicin, changed with the applied membrane potential. However, in the case of bacteriorhodopsin which was fully embedded in the lipid membrane the change in ellipticity was the same at the membrane potential in the two directions while in the case of alamethicin the change in ellipticity with potential is assymetric (Fig. 10a and b). The difference stems from the fact that the degree of embedding of alamethicin into the lipid bilayer is a function of the potential and of its direction.

4. Lateral mobility of photosystem I on the surface of inflated thylakoid vesicles

Upon application of direct electric field pulses on a suspension of vesicles containing charged surface components, electrophoretic mobility is induced. Vesicles move with respect to the solution and each charged component on the vesicular surface moves with respect to its environment and eventually accumulates on one pole of the vesicle while it is depleted on the other one. Diffusion counteracts this accumulation and when the field pulses are stopped the charged components redistribute uniformly in a diffusion controlled way. The charged component on the (thylakoid vesicle investigated by us was photosystem I (PSI). To monitor the redistribution of PSI particles during and after electrophoresis was made use of the spatial characteristics of the electrophotoluminescence (EPL) originating from it. The EPL originates from the hemisphere of the vesicles at which the induced electrical field (20-30 time the amplitude of the field used for electrophoresis) destabilizes the photoinduced charge separation [10]. Thus as shown in Fig. 11 we obtain an enhancement of EPL when the destabilizing field acts on the hemisphere where there is an accumulation of PSI and diminution of EPL it acts on the hemisphere depleted of PSI.

These experiments could be carried before appreciable rotation of the vesicles as the rotational time constant of the large vesicles was above 10 min, while the electrophoretic mobility was completed within 10 sec and the back diffusion within 2-3 min.

The average apparent electric mobility, determined from the time course of EPL on one hemisphere or its decrease on the other one as a function of prepulse length and intensity was of the order of $3 \cdot 10^{-5} \text{ cm}^2 \text{ V}^{-1} \text{ sec}^{-1}$. The assymetric distribution of the PSI reached a steady state when the diffusional, electrostatic and elastic forces balanced the electrophoretic driving force. A lateral diffusion coefficient of $\sim 5 \cdot 10^{-9} \text{ cm}^2 \text{ sec}^{-1}$ was

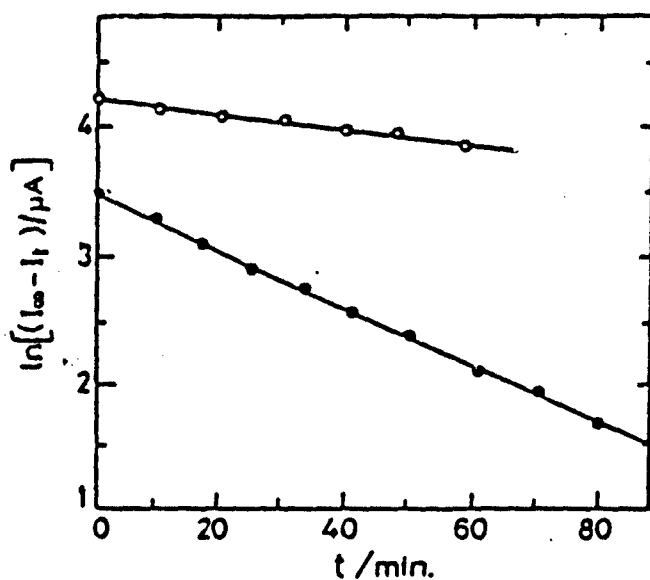


Fig 9. Linear dependence of $\ln(I_{\infty} - I_t)$ on time from vesicles containing 3% GM1. Inner initial salt concentration 0.05 M Na_2SO_4 + 0.05 M Ti_2SO_4 . Outer concentration 0.1 M Na_2SO_4 . (○—○) 40 $\mu\text{g}/\text{ml}$ lipid vesicles of ~ 300 nm diameter, 2.5×10^{-9} M valinomycin, 0.4 $\mu\text{g}/\text{ml}$ CT. (●—●) 100 $\mu\text{g}/\text{ml}$ lipid vesicles, 5×10^{-8} M valinomycin and 1 $\mu\text{g}/\text{ml}$ CT.

Best Available Copy

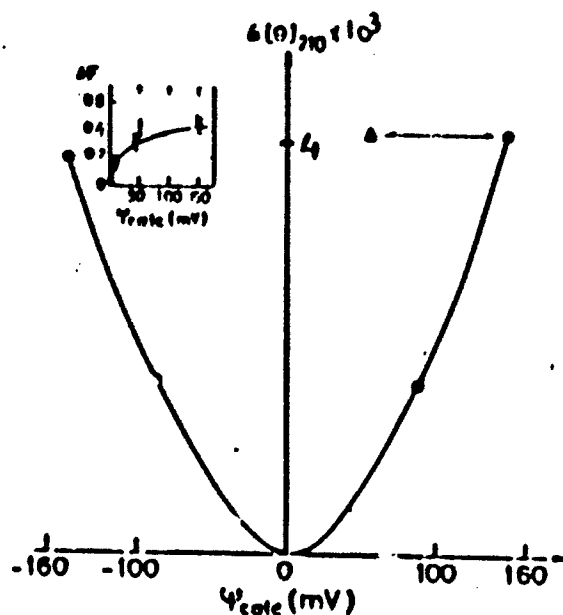


FIGURE 10a The dependence of the ellipticity of bacteriorhodopsin reconstituted in vesicles on the electric diffusion potentials. Ordinate: the decrease of the C.D. signal at 210 nm induced by 10^{-7} M valinomycin. Abscissa: electrical potentials calculated by Nernst equation. The sign indicates the polarity inside the vesicle. The triangle is set at the potential measured by fluorescence quenching of DiSC₂(5) instead of the potential calculated by the Nernst equation (1.6 mV) as indicated in the figure. (Insert) calibration curve of the fluorescence quenching of DiSC₂(5) dye as a function of the Nernst potential in pure lipid (80% PC 20% PS) vesicles in the presence of K^+ gradient and 10^{-7} valinomycin. The potential for the bacteriorhodopsin containing vesicles is indicated with an arrow.

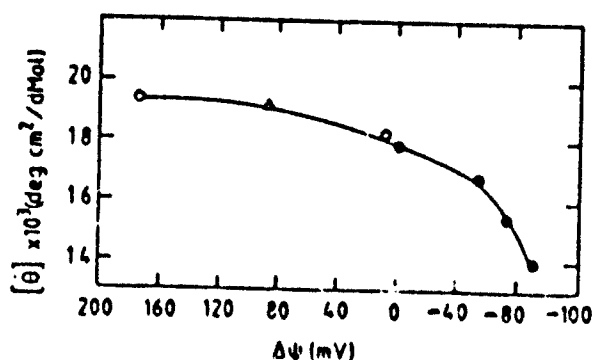
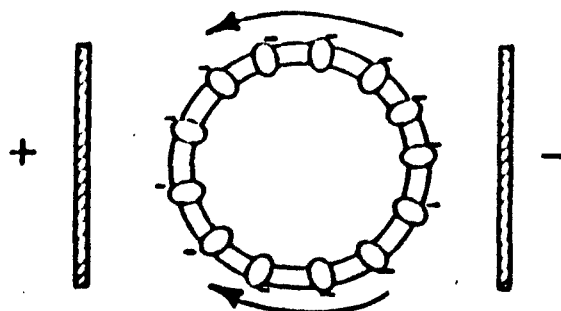


Fig. 10b The molar ellipticity of alamethicin as function of Donnan potential calculated from Eqn. 2. The experimental points were obtained by PA^- addition outside the vesicles (●), by preparing the vesicles with 0.1 M PA^- and then dialyzing against NaCl (○) or by adding PEI^+ outside the vesicles (Δ). See text for details about generating the electric field.

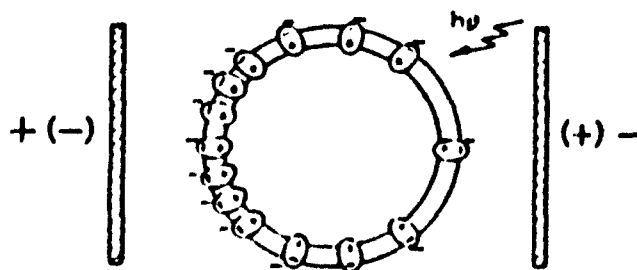
Determination of electrophoretic mobility of photosystem I

13

A Polarization by low electric field prepulses



B Charge separation upon illumination and induced luminescence by high electric field pulse (EPL)



C EPL traces

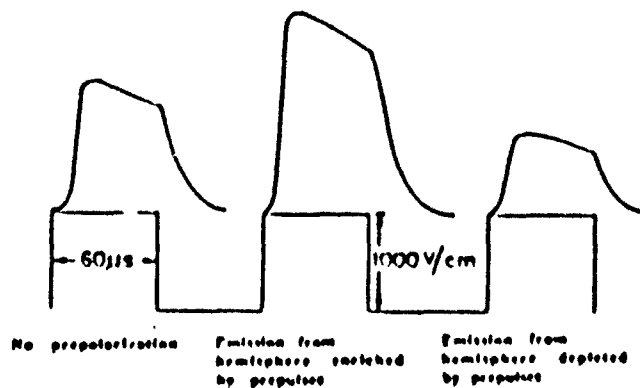


FIGURE 11 Scheme of the experimental procedure. (A) Electrophoretic propagation of PS I particles along the surface of the vesicle, causing accumulation on one pole and depletion on the other one. (B) EPL from depleted or the enriched (electrode signs in brackets) hemispheres. (C) EPL traces: (a) without prepulse, (b) EPL from the enriched hemisphere; (c) EPL from depleted hemisphere.

Best Available Copy

found for the PSI complex from the diffusional relaxation after cessation of the electric field pulse train. Between 23 and 150 electron charges per moving particle were estimated from the electrophoretic mobility. 14

5. Work that has been started

a. Conformation changes in the lipid layer.

We failed to detect by CD or FTIR any conformational changes in lipid layers upon application of electric field. We decided therefore to monitor the conformational changes by these methods where conformational changes are inferred from other physical properties e.g. when cholesterol is added to phospholipids. Indeed the shifts in frequencies and intensities of stretching and bending of CH₂ and of CO bands of the phospholipid is relatively small (see ref. by Brumfeld et al., submitted) and only negligible shifts are expected by lesser perturbations. The amide bands of sphingolipids give amide bands in IR and CD spectra which are strongly dependent on the phase and the conformation in pure lipids. We started determining these spectra and their change during phase transition when diluting the sphingolipids by phospholipids.

b. How does membrane potential affect flip flop of membrane lipids?

This is an important question when one thinks about the asymmetric lipid distribution in biological membranes. To tackle the problem we started measuring the time dependence of the external charge of vesicles composed of different ratios of PC to phosphatidylserine (PS) after applying membrane potentials of different size and direction.

References

1. Allen, R.C. (1983) Sulfonamide diuretics. In: Diuretics. E.J. Cragoe, ed. pp. 49-200. J. Wiley, N.Y.
2. Pagano, R.E. and Miller, I.R. (1973) J. Coll. Int. Sci. 45:126.
3. Fishman, P.H. (1982) J. Memb. Biol. 69:65.
4. Nishuka, Y. (1986) Science 233:305-312.
5. LeCompte, M.-F. and Miller, I.R. (1980) Biochem. 19:3439.
6. Pandey, R.C., Cook, J.C. and Rinehart, K.L. (1977) J. Am. Chem. Soc. 99:8469.
7. Habermann, E. and Jentsch, J. (1969) Hoppe Seiler Z. Physiol. Chem. 348:37.
8. Deamer, D.D. and Bangham, A.D. (1976) Biochim. Biophys. Acta 443:629.
9. Miller, I.R. (1985) Biochim. Biophys. Acta 817:119.
10. Farkas, D.L., Korenstein, R. and Malkin, S. (1984) Biophys. J. 45:363.

List of publications of the work supported by the ONR grant

1. Brumfeld, V. and I.R. Miller (1988) Effect of membrane potential on the conformation of bacteriorhodopsin reconstituted in lipid vesicles. Biophys. J. 54:747-750.
2. Miller, I.R. and E. Yavin (1988) The effect of interactions in the head groups on monolayer structure and permeability. Bioelectrochem. Bioenerg. 19:557-567.

3. Miller, I.R., H. Vinkler and E. Yavin (1989) Cholera toxin complexes with the ganglioside GM1 in lipid monolayers and bilayers. Effect on structure and permeability. *Bioelectrochem. Bioenerg.* 22:365-377.
4. Brumfeld, V. and I.R. Miller and R. Korenstein. (1989) Electric field induces lateral mobility of photosystem I in the photosynthetic membrane. A study by electrophotoluminescence. *Biophys. J.* 56:607-614.
5. Brumfeld, V. and I.R. Miller (1990) Electric field dependence of alamethicin channels. *Biochim. Biophys. Acta.* 1024:49-53.
6. Brumfeld, V. and Lester, D.S. (1990) Protein kinase C penetration into lipid bilayers. *Arch. Biochem. Biophys.* 277:318-323.
7. Lester, D.S., L. Doll, V. Brumfeld and I.R. Miller (1990) Lipid dependence of surface conformations of protein kinase C. *Biochim. Biophys. Acta.* 1039:33-41.
8. Miller, I.R. and L. Doll. Adsorption of alamethicin and melittin on base and phospholipid covered mercury electrodes. *Bioelectrochem. Bioenerg.* 24: in press.
9. Miller, I.R. and L. Doll. Release of ions from large unilamellar vesicles by alamethicin and by melittin. *Bioelectrochem. Bioenerg.* Submitted.
10. Brumfeld, V., D. Bach and I.R. Miller. FTIR spectroscopy of aqueous dispersions of phosphatidylserine-cholesterol mixture. Submitted.

Best Available Copy